Literature Review

Joshua Torrance

May 10, 2012

1 Introduction

The University of Melbourne's cold-atom electron source aims to be able to create high-brightness, high-coherence electron bunches for use in coherent electron diffractive imaging. The imaging of nanoscale objects such as biological molecules [1, 2] and defects in solid-state devices [3] by ultrafast, single-shot electron diffractive imaging would provide important information about structure and dynamic processes of these nanoscale objects.

In order to determine the structure of biological molecules atomic, subnanometre imaging resolution is required. A number of techniques are available for determining these structures [4–6] and the most successful to date has been x-ray crystallography [7, 8]. Unfortunately the process of crystallising biological proteins such as membrane proteins is difficult and to date relatively few have been successfully crystallised [9].

Membrane proteins are the proteins that are associated with or attached to the membrane of a cell. They are involved in detecting and conveying external signals into cells which allows the cell to interact with and respond to their environment [10]. Membrane proteins are important in determining immune responses, interactions with pharmaceuticals, cell adhesion to form tissues and in controlling important metabolic processes such as salt balance, energy production and photosynthesis [11]. Determining the structure of these molecules is a key step in understanding their chemical and biological function. The importance of knowing the atomic structure of biomolecules is exemplified by the enormous progress made in various fields of biology once the double-helical structure of DNA was determined from x-ray images in 1953 [12]. Once a protein's structure and function are known then it becomes possible to design drugs [13] where needed and to more fully understand how the protein behaves in its biological system.

New imaging techniques and light sources such as x-ray free electron lasers and ultrafast single-shot diffraction have been driven by the goal of overcoming the limitations of x-ray crystallography. Ultrafast single-shot diffraction imaging also has the potential to determine the dynamic structure of biological molecules.

1.1 Ultrafast, single-shot, coherent diffractive imaging with electrons

X-ray diffraction from crystals was first observed a century ago [14] and resulted in a Nobel prize being awarded to William Bragg and his son. Since then coherent diffractive imaging (CDI) has been performed on a myriad of different samples with coherent beams of x-rays and electrons.

Electron interactions with molecules are significantly strong than those of x-rays. For similar energies the electron interaction with a sample is $10^5 - 10^6$ higher than that of x-rays [15].

1.1.1 Single-shot diffractive imaging

Single-shot diffractive imaging with an x-ray source of sufficient brightness should be able to produce a diffraction pattern from scattered x-rays from a single molecule before the molecule is destroyed by the Coulomb explosion which follows photoionisation within the molecule [16, 17]. Single-shot imaging aims to avoid the need for crystallisation with x-ray imaging since with a sufficiently bright source imaging of any molecule would be possible.

With femtosecond timescale single-shot imaging it is possible to observe such things as molecular vibration and dynamic chemical processes [18]. With the sophisticated imaging techniques currently in development it will become possible to create "molecular movies" [1] of these processes.

1.2 Melbourne cold-atom electron source

The University of Melbourne's cold-atom electron source project aims to produce an electron source for coherent diffractive imaging. If bright, coherent, femtosecond long bunches of electrons can be produced then CDI can be performed on a range of structures.

In order to produce the electrons Rubidium atoms from an oven are first slowed using a Zeeman slower which consists of a near-resonant laser beam and a tapered magnetic coil. The Zeeman slower slows the atoms leaving the oven from speeds of order 300m/s to speeds of order 10m/s which correspond to a few Kelvin.

The slowed atoms are then cooled and trapped in a magneto-optic trap which consists of three sets of counter-propagating, circularly polarised, near-resonant laser beams combined with a magnetic field generated by two mag-

netic coils in an anti-Helmholtz arrangement. This serves to cool and trap the atoms to a temperature of order 100 μK forming an ultra-cold atom-cloud.

With the atom cloud produced the electron beam production can begin. The cloud is first illuminated by a resonant 780 nm excitation laser to excite the valance electrons to a high energy level followed by a 480 nm ionisation laser pulse which provides just enough energy to ionise the electrons. Since the electrons are have little or no excess energy once they have been ionised they are considered to be 'cold'.

These cold electrons are then accelerated out of the cloud by a uniform electric field, guided to the neighbouring sample chamber and focused onto the target sample. After passing through the sample the resulting diffraction pattern is incident upon the detector.

The diffraction pattern recorded by the detector can be used to determine the structure of the sample.

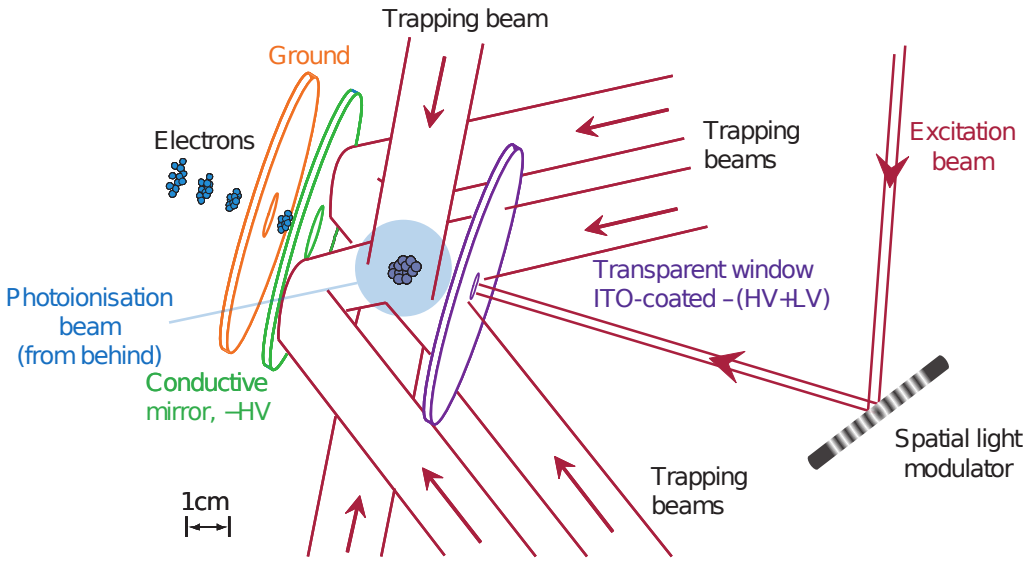

Figure 1: A quasi mirror MOT is used to trap Rb atoms. The atoms are then ionised and the resulting electrons are accelerated using two parallel plates.

2 Motivation for an optical dipole trap

When extracting the ionised electrons from the atom cloud it is necessary to turn off the magnetic trapping fields and the magnetic fields of the Zeeman slower in order to prevent magnetic distortions of the electron bunch trajectory. This means that just before electron extraction the cloud is no longer trapped it begins to expand. The use of additional trapping mechanisms that do not interfere with the electron trajectories, such as an optical dipole trap (ODT), will help prevent this expansion. An ODT will also serve to stabilise the initial position of the electron bunches which tend to drift at present due to dispersal of currents, and hence magnetic fields, in the magnetic coils and their power supplies.

Using an ODT in this system should also allow an increase in the brightness and perhaps coherence of the source due to higher atom cloud densities during the ionisation process.

2.1 Brightness

Brightness is important in single-shot CDI due to the need to maximise the scattered signal to ensure sufficient sampling of the specimen within the exposure time.

For the cold-atom source the transverse brightness at the source is given by [19]

$$B_{\perp} = \frac{I_p m_e c^2}{4\pi^2 \sigma_x \sigma_y k_B T}, \tag{1}$$

where σ_x and σ_y are the root mean squared source size along the respective axes, I_p is the peak electron current and T is the source temperature.

The brightness of an electron bunch can be increased by a reduction in the length of the bunch or by increasing the density. A short bunch is also necessary for ultrafast electron diffraction.

The use of an ODT will increase the density of the atom-cloud by trapping the otherwise expanding atom-cloud which will result in an increase of the electron bunch density and hence the brightness.

2.2 Coherence

Unsurprisingly coherence is an important factor in CDI since this technique relies on the interference of the diffracted waves. The transverse coherence

length of a imaging beam must be approximately twice the width of the object being imaged [20] in order to properly resolve structure.

For a quasi-homogeneous source [21], the transverse coherence length L_c can be related to the transverse momentum spread, and hence the temperature, through [22]

$$L_c = \hbar/\sqrt{m_e k_B T}. \tag{2}$$

The transverse coherence is determined solely from the temperature of the electrons which is proportional to the temperature of the electron source and the ionisation energy.

The coherence of the electron bunches could be increased with the sophisticated use of ODTs since the trap would serve to reduce the temperature of the atom cloud, and hence the electron bunches.

3 Optical Dipole Trapping

The use of ODTs in the cold-atom electron source will allow greater stability of the atom cloud during ionisation and extraction as well as increasing the density of the atom cloud during these phases.

3.1 History of optical dipole trapping

The use of the optical dipole force as a confining mechanism was first proposed by Askar'yan in 1962 [23] for plasmas and neutral atoms. Ashkin successfully demonstrated the trapping of micron-size latex spheres suspended in water using a focused Gaussian lasers in 1970 [24]. The first optical trapping of atoms was demonstrated by Chu et. al. in 1986 [25] where a ODT was used to trap sodium atoms.

Since then ODTs have been used extensively in atom optics especially in the creation of Bose-Einstein condensates (BECs) and atom lasers.

3.2 Theory of Dipole Trapping

ODTs are sometimes considered to be the simplest form of atom trap for two-level atoms since they consist solely of a focused, Gaussian laser beam detuned from the atomic resonances. The intensity of the Gaussian laser beam at the beam waist varies transversely with r as

$$I(r) = I_0 e^{-r^2/w_0^2}, \tag{3}$$

where I_0 is the intensity at the centre of the beam at the waist, r is the radial distance from the centre of beam and w_0 is the beam radius at the focus.

The ground state light shift for ground state atoms in the laser field is given by [26]

$$\Delta E_g = \frac{\hbar \Omega^2}{4\delta}, \tag{4}$$

where the Rabi frequency $\Omega^2 = \gamma^2 I/2I_s$ and γ is the linewidth, I is the light intensity and I_s is the saturation intensity. Thus the light shift is larger at points of high intensity such as the centre of the beam and the beam focus.

In order to trap the laser is detuned below the resonances such that $\delta = \omega_l - \omega_a < 0$ where ω_l is the laser frequency and ω_a is the atomic resonance frequency. With negative detuning the ground-state light shift is negative

everywhere and thus atoms feels a force towards the centre given by the gradient of the light shift, and for $\delta \gg \Omega$ and $\delta \gg \gamma$ the force is given by

$$F \simeq -\frac{\hbar}{4\delta}\nabla(\Omega(r)^2) = -\frac{\hbar\gamma^2}{8\delta I_s}\nabla I(r). \tag{5}$$

At the focus of a Gaussian beam this force is

$$F \simeq \frac{\hbar\gamma^2}{4\delta}\frac{I_0}{I_s}\frac{r}{w_0^2}e^{-r^2/w_0^2}, \tag{6}$$

and thus the transverse trapping potential is given by

$$U = -\int dr F \simeq \frac{\hbar\gamma^2}{8\delta}\frac{I_0}{I_s}e^{-r^2/w_0^2}. \tag{7}$$

It is easy to see with this equation how a negative (red) detuning will result in an inwards, trapping force and a positive (blue) detuning will result in a outwards, repulsive force. Blue detuned lasers can be used for trapping if the beam has a low intensity centre however [27–30].

3.2.1 Scattering rates

Atoms in near-resonant light fields experience a non-conservative force due to excitation and spontaneous decay (ie. scattering). More general expressions for the trapping potential can be used to compare the trap potential to the scattering rate due to the photon absorption [31]

$$U_{dip}(\vec{r}) = \frac{3\pi c^2}{2\omega_0^3}\frac{\gamma}{\delta}I(\vec{r}) \tag{8}$$

$$\Gamma_{sc}(\vec{r}) = \frac{3\pi c^2}{2\hbar\omega_0^3}\left(\frac{\gamma}{\delta}\right)^2 I(\vec{r}) \tag{9}$$

The scattering rate should be kept to a minimum in order to prevent the heating atoms in the trap. Fortunately the relationships are such that for large detunings $U_{dip} \gg \Gamma_{sc}$. Such far detuned lasers however do create shallower traps and thus require more powerful lasers to create similar trap depths.

3.3 Using an optical dipole trap in a cold-atom electron source

An ODT can serve several purposes in the cold-atom electron source including increasing the brightness and coherence of the electron bunches as described earlier.

A number of design choices in the development of this dipole trap are under consideration such as the wavelength of the trap, the configuration of the trapping beam/s and the size of the beam waist.

3.3.1 Available equipment

Two main options are available as far as light sources for the trap,

- a 20mW, 780nm diode laser amplified by a tapered amplifier (TA) to 1.8W,
- a 20W, 1064nm fibre laser.

The 780nm diode laser that seeds the TA can be tuned away from the 780nm resonance by tens of nanometres however the TA has a maximum wavelength of 785nm. This restricts the possible red detuning to a maximum of 5nm.

The 1064nm laser is extremely far away from the resonances which results in reduced scattering rates however lasers with powers as high as 20W require more caution in their use as well as suitable optics capable of dealing with the high-intensity light.

3.3.2 1064nm optical dipole traps

ODTs with a wavelength near 1064nm are frequently used when rubidium BECs are being formed [32–37]. These BECs are used for many different applications including the creation of atom-lasers [32–34], atomic clocks [38] and obviously further studies into BECs themselves and related trapping mechanisms [35–37].

ODTs with wavelengths at 1064nm are not only used in rubidium BECs. They have to used to form BECs of caesium [39], chromium [40], double-species BECs [41], and even molecular BECs [42].

3.3.3 "Near" 780nm optical dipole traps

Traps made from lasers "near" 780nm are more often used when studying and developing trapping methods. Such traps have detunings that vary from 0.5nm [43] to over 60nm [44,45] and are usually referred to as far-off-resonance traps (FORTs). Some of the things that these laser have been used to study are dipole trap loading [46], trapping single atoms [45] and the combination of an ODT with Sisyphus cooling [43].

3.3.4 Configurations

The simplest ODT consists simply of a focused Gaussian beam [25] and many of the references use this simple configuration.

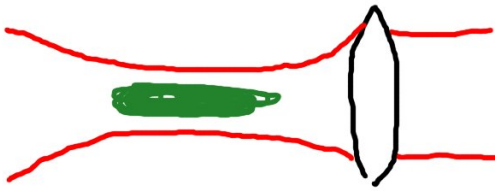

Figure 2: A simple ODT configuration

Crossed dipole traps [36, 37, 47, 48] are a more complicated configuration that can provide a stronger trap as well as control over the shape of the trap and the trapping potentials in various directions. Unlike simple dipole traps which create long cigar-shaped traps crossed dipole traps can create spherical traps.

Crossed dipole traps do not require the beams to be at right angles. For example Couvert et. al. [33] have their beams at 45 degrees when generating atom lasers.

Kinoshita et. al. [49] use a crossed dipole configuration where the two beams do not cross at their respective foci. Instead the beams are crossed at the desired beam waist (initially 300μm in this case) after which the waists at the trapping point can be dynamically controlled by adjusting the positions of the lens.

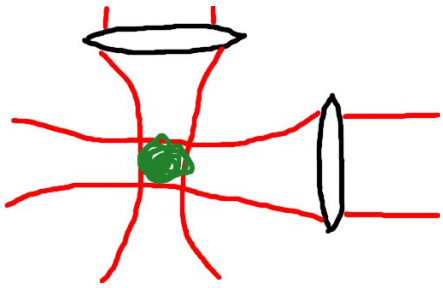

Figure 3: A crossed ODT configuration

3.3.5 Waist size

The size of the beam waist is an important factor for the performance of ODTs. In most experiments involving dipole traps the beam waist used is in the region of 30μm in order to provide the deepest trap possible. For the cold-atom electron source however it may be desirable to use a broader trap in order to trap a larger number of atoms. Then again the deepest trap attainable may provide better results.

In order to provide an easily modifiable beam waist a setup like the one describe in figure 4 which consists of a beam expander consisting of a concave then convex lens followed by the focusing lens could be used.

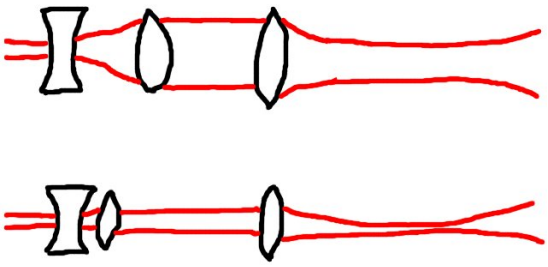

Figure 4: An example setup for controlling the beam waist

This configuration allows manipulation of the size of the beam incident on the final lens by adjusting the distance between the lens in the beam

expander. This in turn changes the beam waist at the focus according to

$$2w_0 = \frac{4\lambda}{\pi}\frac{f}{d} \tag{10}$$

where w_0 is the beam radius at the focus, λ is the wavelength of the light, f is the focal length of the final lens and d is the diameter illuminated by the beam incident on the final lens.

References

[1] J. R. Dwyer, C. T. Hebeisen, R. Ernstorfer, M. Harb, V. B. Deyirmenjian, R. E. Jordan, and R. J. Dwayne Miller. Femtosecond electron diffraction: 'making the molecular movie'. *Philosophical Transactions of the Royal Society A: Mathematical, Physical and Engineering Sciences*, 364(1840):741–778, March 2006.

[2] J. C. Williamson, J. Cao, H. Ihee, H. Frey, and A. H. Zewail. Clocking transient chemical changes by ultrafast electron diffraction. *Nature*, 386(6621):159–162, March 1997.

[3] B. J. Siwick, J. R. Dwyer, R. E. Jordan, and R. J. Dwayne Miller. An Atomic-Level view of melting using femtosecond electron diffraction. *Science*, 302(5649):1382–1385, November 2003.

[4] J. E Nettleship, J. Brown, M. R. Groves, and A. Geerlof. Methods for protein characterization by mass spectrometry, thermal shift (ThermoFluor) assay, and multiangle or static light scattering. *Methods in Molecular Biology (Clifton, N.J.)*, 426:299–318, 2008. PMID: 18542872.

[5] D. I. Svergun and M. H. J. Koch. Small-angle scattering studies of biological macromolecules in solution. *Reports on Progress in Physics*, 66(10):1735–1782, October 2003.

[6] S. J. Opella and F. M. Marassi. Structure determination of membrane proteins by NMR spectroscopy. *Chemical Reviews*, 104(8):3587–3606, August 2004. PMID: 15303829.

[7] J. C. Kendrew, G. Bodo, H. M. Dintzis, R. G. Parrish, H. Wyckoff, and D. C. Phillips. A Three-Dimensional model of the myoglobin molecule obtained by X-Ray analysis. *Nature*, 181(4610):662–666, March 1958.

[8] I. Usón and G. M. Sheldrick. Advances in direct methods for protein crystallography. *Current Opinion in Structural Biology*, 9(5):643–648, October 1999. PMID: 10508770.

[9] A. Geerlof, J. Brown, B. Coutard, M. P. Egloff, F. J. Enguita, M. J. Fogg, R. J. C. Gilbert, M. R. Groves, A. Haouz, J. E. Nettleship, P. Nordlund, R. J. Owens, M Ruff, S. Sainsbury, D. I. Svergun, and

M. Wilmanns. The impact of protein characterization in structural proteomics. *Acta Crystallographica. Section D, Biological Crystallography*, 62(Pt 10):1125–1136, October 2006. PMID: 17001090.

[10] M. S. Almén, K. J. V. Nordström, R. Fredriksson, and H. B. Schiöth. Mapping the human membrane proteome: a majority of the human membrane proteins can be classified according to function and evolutionary origin. *BMC Biology*, 7(1):50, August 2009.

[11] D. D. Chiras. *Human Biology*. Jones & Bartlett Learning, August 2011.

[12] J. D. Watson and F. H. C. Crick. Molecular structure of nucleic acids: A structure for deoxyribose nucleic acid. *Nature*, 171(4356):737–738, April 1953.

[13] L. H. Pinto, L. J. Holsinger, and R. A. Lamb. Influenza virus M2 protein has ion channel activity. *Cell*, 69(3):517–528, May 1992.

[14] W. H. Bragg. X-rays and crystals. *Nature*, 90:219, October 1912.

[15] G. Sciaini and R. J. Dwayne Miller. Femtosecond electron diffraction: heralding the era of atomically resolved dynamics. *Reports on Progress in Physics*, 74(9):096101, September 2011.

[16] R. Henderson. The potential and limitations of neutrons, electrons and x-rays for atomic resolution microscopy of unstained biological molecules. *Quarterly Reviews of Biophysics*, 28(2):171–193, May 1995. PMID: 7568675.

[17] R. Neutze, R. Wouts, D. van der Spoel, E. Weckert, and J. Hajdu. Potential for biomolecular imaging with femtosecond x-ray pulses. *Nature*, 406(6797):752–757, August 2000.

[18] A. H. Zewail. 4d ultrafast electron diffraction, crystallography, and microscopy. *Annual Review of Physical Chemistry*, 57(1):65–103, 2006.

[19] M. Reiser. *Theory and Design of Charged Particle Beams*. John Wiley & Sons, August 2008.

[20] J. C. H. Spence, U. Weierstall, and M. Howells. Coherence and sampling requirements for diffractive imaging. *Ultramicroscopy*, 101(2-4):149–152, November 2004. PMID: 15450660.

[21] K. A. Nugent. Coherent methods in the x-ray sciences. *Advances in Physics*, 59(1):1–99, 2009.

[22] T. van Oudheusden, E. F. de Jong, S. B. van der Geer, W. P. E. M. op't Root, O. J. Luiten, and B. J. Siwick. Electron source concept for single-shot sub-100 fs electron diffraction in the 100 keV range. *Journal of Applied Physics*, 102(9):093501–093501–8, November 2007.

[23] G. Askar'yan. Effects of the gradient of a strong electromagnetic beam on electrons and atoms. *Soviet Physics - Journal of Experimental and Theoretical Physics*, 15(1088), 1962. INSPEC:10786990.

[24] A. Ashkin. Acceleration and trapping of particles by radiation pressure. *Physical Review Letters*, 24(4):156–159, January 1970.

[25] S. Chu, J. E. Bjorkholm, A. Ashkin, and A. Cable. Experimental observation of optically trapped atoms. *Physical Review Letters*, 57(3):314–317, July 1986.

[26] H. J. Metcalf and P. van der Straten. *Laser Cooling and Trapping*. Springer, 1999.

[27] N. Davidson, H. Jin Lee, C. S. Adams, M. Kasevich, and S. Chu. Long atomic coherence times in an optical dipole trap. *Physical Review Letters*, 74(8):1311–1314, February 1995. PMID: 10058988.

[28] H. J. Lee, C. S. Adams, M. Kasevich, and S. Chu. Raman cooling of atoms in an optical dipole trap. *Physical Review Letters*, 76(15):2658–2661, April 1996.

[29] R. Ozeri, L. Khaykovich, and N. Davidson. Long spin relaxation times in a single-beam blue-detuned optical trap. *Physical Review A*, 59(3):R1750–R1753, March 1999.

[30] N. Friedman, L. Khaykovich, R. Ozeri, and N. Davidson. Compression of cold atoms to very high densities in a rotating-beam blue-detuned optical trap. *Physical Review A*, 61(3):031403, February 2000.

[31] R. Grimm, M. Weidemüller, Y. B. Ovchinnikov, Benjamin Bederson, and Herbert Walther. Optical dipole traps for neutral atoms. In *Advances In Atomic, Molecular, and Optical Physics*, volume Volume 42, pages 95–170. Academic Press, 2000.

[32] A. P. Chikkatur, Y. Shin, A. E. Leanhardt, D. Kielpinski, E. Tsikata, T. L. Gustavson, D. E. Pritchard, and W. Ketterle. A continuous source of Bose-Einstein condensed atoms. *Science*, 296(5576):2193–2195, June 2002.

[33] A. Couvert, M. Jeppesen, T. Kawalec, G. Reinaudi, R. Mathevet, and D. Guéry-Odelin. A quasi-monomode guided atom laser from an all-optical Bose-Einstein condensate. *EPL (Europhysics Letters)*, 83(5):50001, September 2008.

[34] G. Kleine Büning, J. Will, W. Ertmer, C. Klempt, and J. Arlt. A slow gravity compensated atom laser. *Applied Physics B: Lasers and Optics*, 100(1):117–123, 2010.

[35] Y.-J. Lin, A. R. Perry, R. L. Compton, I. B. Spielman, and J. V. Porto. Rapid production of ^{87}Rb Bose-Einstein condensates in a combined magnetic and optical potential. *Physical Review A*, 79(6):063631, June 2009.

[36] K. J. Arnold and M. D. Barrett. All-optical Bose–Einstein condensation in a 1.06 μm dipole trap. *Optics Communications*, 284(13):3288–3291, June 2011.

[37] Zhengkun Fu, Pengjun Wang, Shijie Chai, Lianghui Huang, and Jing Zhang. Bose-Einstein condensate in a light-induced vector gauge potential using 1064-nm optical-dipole-trap lasers. *Physical Review A*, 84(4):043609, October 2011.

[38] G. Kleine Büning, J. Will, W. Ertmer, E. Rasel, J. Arlt, C. Klempt, F. Ramirez-Martinez, F. Piéchon, and P. Rosenbusch. Extended coherence time on the clock transition of optically trapped rubidium. *Physical Review Letters*, 106(24):240801, June 2011.

[39] C.-L. Hung, X. Zhang, N. Gemelke, and C. Chin. Accelerating evaporative cooling of atoms into Bose-Einstein condensation in optical traps. *Physical Review A*, 78(1):011604, July 2008.

[40] Q. Beaufils, R. Chicireanu, T. Zanon, B. Laburthe-Tolra, E. Maréchal, L. Vernac, J.-C. Keller, and O. Gorceix. All-optical production of chromium Bose-Einstein condensates. *Phys. Rev. A*, 77(6):061601, June 2008.

[41] G. Thalhammer, G. Barontini, L. De Sarlo, J. Catani, F. Minardi, and M. Inguscio. Double species Bose-Einstein condensate with tunable interspecies interactions. *Physical Review Letters*, 100(21):210402, May 2008.

[42] M. W. Zwierlein, C. A. Stan, C. H. Schunck, S. M. F. Raupach, S. Gupta, Z. Hadzibabic, and W. Ketterle. Observation of Bose-Einstein condensation of molecules. *Physical Review Letters*, 91(25):250401, December 2003.

[43] Kurt W. Miller, Stephan Dürr, and Carl E. Wieman. rf-induced sisyphus cooling in an optical dipole trap. *Physical Review A*, 66(2):023406, 2002.

[44] J. D. Miller, R. A. Cline, and D. J. Heinzen. Far-off-resonance optical trapping of atoms. *Physical Review A*, 47(6):R4567–R4570, June 1993.

[45] M. Weber, J. Volz, K. Saucke, C. Kurtsiefer, and H. Weinfurter. Analysis of a single-atom dipole trap. *Physical Review A*, 73(4):043406, April 2006.

[46] S. J. M. Kuppens, K. L. Corwin, K. W. Miller, T. E. Chupp, and C. E. Wieman. Loading an optical dipole trap. *Physical Review A*, 62(1):013406, June 2000.

[47] M. D. Barrett, J. A. Sauer, and M. S. Chapman. All-Optical formation of an atomic Bose-Einstein condensate. *Physical Review Letters*, 87(1):010404, June 2001.

[48] D. Xiong, P. Wang, Z. Fu, S. Chai, and J. Zhang. Evaporative cooling of ^{87}Rb atoms into Bose-Einstein condensate in an optical dipole trap. *Chinese Optics Letters*, 8(7):627–629, July 2010.

[49] T. Kinoshita, T. Wenger, and D. S. Weiss. All-optical Bose-Einstein condensation using a compressible crossed dipole trap. *Physical Review A*, 71(1):011602, January 2005.